Solar Energy Materials and Solar Cells xxx (xxxx) xxx–xxx

Contents lists available at ScienceDirect

Solar Energy Materials and Solar Cells

journal homepage: www.elsevier.com/locate/solmat

Synthesis and electrochromic properties of conducting polymers: Polyaniline directly grown on fluorine-doped tin oxide substrate via hydrothermal techniques

Jia Chu*, Dengyu Lu, Bohua Wu, Xiaoqin Wang, Ming Gong, Runlan Zhang, Shanxin Xiong

College of Chemistry and Chemical Engineering, Xi'an University of Science and Technology, Xi'an 710054, China

ARTICLE INFO

Keywords:
Polyaniline
Hydrothermal
Electrochromic

ABSTRACT

Inspired by hydrothermal synthesis of inorganic crystallites, we apply one-step hydrothermal polymerization to directly grow polyaniline on fluorine-doped tin oxide (FTO) substrate. In contrast to classical procedure that requires long reaction times and low temperature, hydrothermal polymerization allows for only 3 h under hydrothermal condition. Investigation of the morphology via SEM suggests that PANI fiber aggregates uniformly on FTO substrate. The PANI film was used as electrochromic layer in an electrochromic device and the obtained PANI film shows high electrochromic performance. We believe that this study provided a novel way to directly grow PANI on FTO substrate and, thus, has some impact on the applications of other conjugated polymers in electrochromic and electrochemical devices.

1. Introduction

Conjugated polymers have attracted widespread interest during the last two decades due to their unique electronic, optoelectronic and electrochemical properties [1,2]. Among this type of polymers, Polyaniline (PANI) has attracted special attention due to several reasons: it can be easily prepared by standard oxidation chemical or electrochemical polymerization; it demonstrates higher conductivity and environmental stability and it owns multicolor compared to other conducting polymers [3–5]. During the last three decades PANI became one of the most extensively studied conducting polymers. The different charges, colors and conformation of the multiple oxidation states make the PANI promising for applications in supercapacitors [6–9],sensors [10,11], electrochemical actuators [12], electrochromic devices [13–18] and fuel cells [19,20]. The classical syntheses of PANI are employing oxidative polymerization of aniline or electrochemical syntheses of PANI. PANI of high molecular weight is usually obtained as amorphous products, because they are more difficult to crystalize than small molecules. Little progress has been made in the last decades towards alternative polymerization techniques, e.g., aniline polymerization under X-ray irradiation [21], chemical oxidative polymerization of vaporized aniline monomer on inkjet-printed oxidant patterns [22] and polymerization of aniline in pulsed dc plasma [23]. In spite of the lots amount of reports focused on the choice of oxidants there are few examples of the synthesis focus on the synthesis conditions. For high-performance conducting polymers, nanostructures is a desired feature: it enhances mechanical and thermal strength, or directional properties such as electrical and optical properties. So there is increasing interest in environmental friendly routes to the synthesis of conducting PANI.

The synthesis of PANI can be done in a chemical method to control the growing process. One of the possible approaches to achieve the nanostructures is hydrothermal method. Our approach for the hydrothermal synthesis of PANI is inspired by nature. Hydrothermal method is widely used in the synthesis of inorganic materials, ranging from zeolite synthesis to the artificial crystals. Yet, only few examples exist for the synthesis of organic materials under hydrothermal conditions, mostly dealing with small organic molecules. Recently, several typical polymers synthesized by hydrothermal method have been reported. Zhu and coworkers prepared three polyaniline nanoarchitectures of square nanosheets, microsphere and microdisks using hydrothermal method in the presence of CTAB as a template [24]. Shi synthesized different PANI mesostructures under hydrothermal conditions [25]. Unterlass and coworkers developed highly ordered polyimides via hydrothermal polymerization [26]. The resulting polymer shows superior thermal stability and excellent crystallinity. Hydrothermal polymerization present a fascinating advantage to conventional method: they are carried out in a single step and originally green with water as solvent. Although the syntheses carried out in the water, the polymerization work very well and even lead to highly crystalline polymer. Therefore, hydrothermally-produced conducting PANI has the opportunity to be at the forefront of becoming novel and evolving polymeric materials under high-temperature aqueous solutions at high vapor

* Corresponding author.

http://dx.doi.org/10.1016/j.solmat.2017.05.049
Received 1 December 2016; Received in revised form 27 April 2017; Accepted 20 May 2017

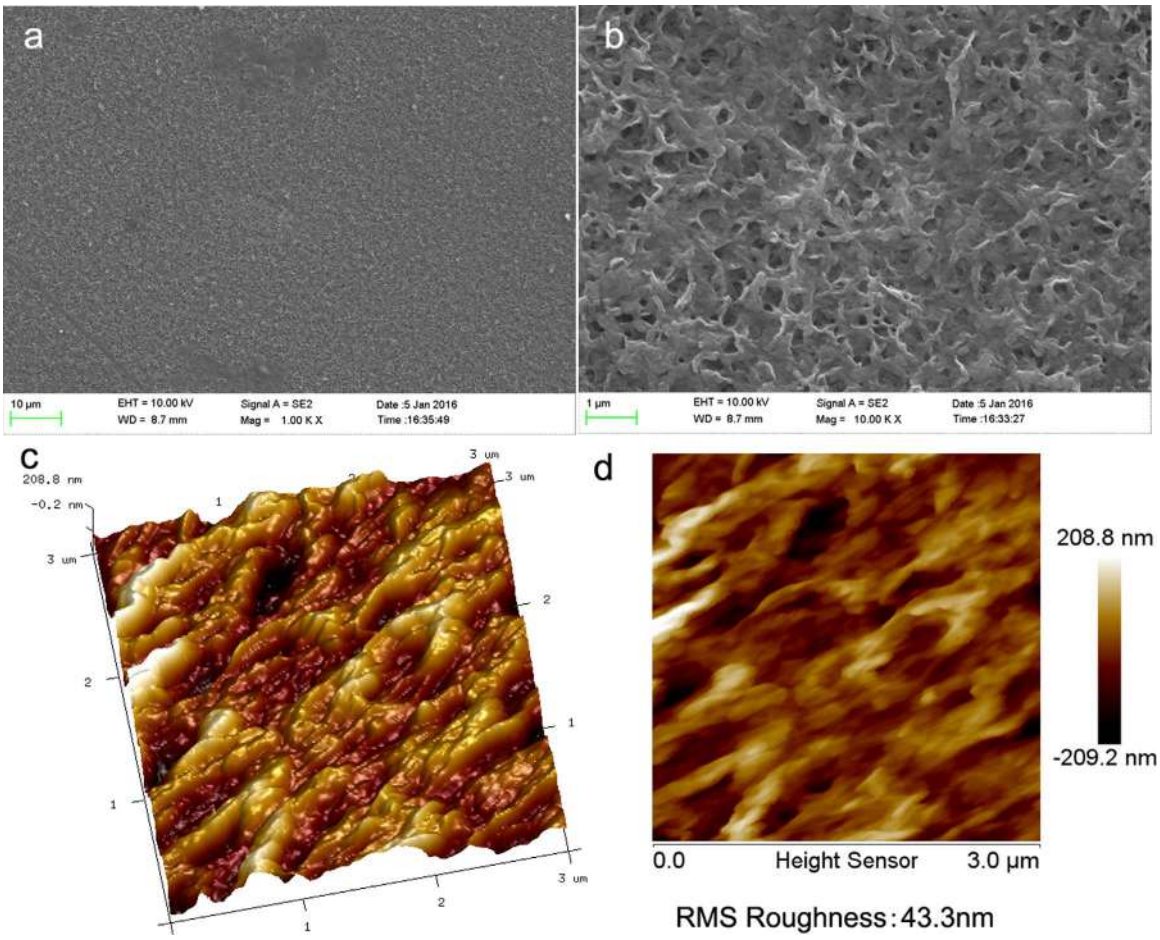

Fig. 1. (a) Surface morphologies of PANI film and (b) high magnification of the PANI film on FTO substrate. AFM images of the surface morphology of (c) 3D and (d) 2D height image with a 1 μm × 1 μm scale.

pressures. So far, relatively little research has been conducted on directly grown PANI on FTO substrate via a simple hydrothermal growth.

Herein, we report a hydrothermal approach that has been developed for synthesis of PANI film on FTO substrate directly by one-pot polymerization of aniline. Our study shows that the PANI are suitable for the build-up of thin films via hydrothermal method, and that the resulting films exhibit interesting electrochromic properties with high contrast and fast switching times.

2. Experiment

2.1. Materials

Aniline was purchased from Aladdin and distilled before use under reduced pressure. Ammonium persulfate($(NH_4)_2S_2O_8$, APS), anhydrous lithiumperchlorate ($LiClO_4$), propylene carbonate (PC),Dodecyl benzenesulfonic acid (DBSA) and Hexadecyltrimethyl ammonium bromide (CTAB) were of analytical grade and used without further purification. All the distilled water was used for sample preparation and characterization. The fluorinetin oxide (FTO) coated glass plates of thickness of 2.2 mm with resistance of 8–12 Ω sq^{-1} were purchased from NSG, Japan, and used as the substrate for PANI film.

2.2. Synthesis

PANI was directly grown on a fluorine-doped tin oxide (FTO) glass substrate using a hydrothermal method. The FTO substrates were cleaned with acetone, ethanol, finally rinsed with deionized water and dried in air. In a typical experimental procedure, 0.7288 g of CTAB was dissolved in 77 mL of H_2O with vigorous stirring to form a uniform solution. Then 0.2 mg of freshly distilled aniline was then added to CTAB solution. After that, 4 mL of DBSA was added to the solution and stirred for 10 min. To this mixture, a solution containing 0.2192 g of APS was slowly added into the monomer solution under vigorous stirring. After that, the entire solution was transferred into a Teflon vessel and the FTO substrate was placed at an angle against the wall of the autoclave with the conductive side facing down. The hydrothermal reaction was conducted at 160 °C for 3 h and then cooled overnight. After rinsed extensively with deionized water and dried in vacuum. The PANI film was uniformly coated on the FTO glass substrate.

2.3. Fabrication of the electrochromic device

The FTO coated with PANI thin film was fabricated as work electrode. The electrochromic devices with sandwiched structure of FTO/electrochromic layer/polymer gel electrolyte/FTO were fabricated according to the methods described in our previous publication [16]. The polymer gel electrolyte used was a mixture of 0.512 g of LiClO4, 2.8 g of PMMA, 8 g of propylene carbonate, and 28 g of acetonitrile.

2.4. Characterization

Scanning electron microscopy (SEM) images of PANI were recorded on a Zeiss Supra 55 field emission scanning electron microscope. Specimens for SEM experiments were made by placing a piece of FTO glass with PANI film on a conducting stage and were then observed with gold coating. The FTIR spectrum was acquired on a Perkin-Elmer

Spectrum 100 Series FTIR spectrometer. Measurements were collected in KBr pellets. Raman spectra were collected on a Renishaw inVia Raman microscope. A 2400 lines mm^{-1} grating was used for all measurements, providing a spectral resolution of ± 1 cm^{-1}. As an excitation source the Ar+ laser (532 nm with less than 0.5 mW laser powers) was used. The laser spot was focused on the sample surface using a long working distance 50x objective. Tapping mode atomic force microscopy (AFM) was performed using Si_3N_4 tip in air at room temperature. Images were captured with scan sizes of 1 and 3 μm at a scan rate of 0.5 Hz, and the surface roughness values of original unprocessed images were evaluated from the scanned surface topography. The cyclicvoltammetry test and electrochemical impedance spectroscopy was carried out on an Autolab PGSTAT302N electrochemical workstation in a three-electrode environment with the PANI film on FTO glass as the working electrode, neat Pt plate as the counter electrode and Ag/AgCl as the reference electrode in a 0.1 M $LiClO_4$/acetonitrile electrolyte solution. The electrochromic behavior of PANI films was examined using an Autolab PGSTAT101 potentiostat with the UV–vis spectrometer (SHIMADZU UV2550). The electrochemical impedance analysis of the film was determined over the frequency range of $10^{-2}-10^{6}$ Hz with a signal amplitude of 5 mV using the same three-electrode electrochemical cell as that for CV tests.

3. Results

The morphology of PANI film grown on FTO glass was investigated by means of a field-emission scanning electron microscopy. Fig. 1a is a low magnification image of PANI film, which reveals that the whole surface of the FTO glass is covered uniformly with PANI film. As shown in Fig. 1b, the PANI film is aligned to FTO substrate with PANI nanofiber aggregation to form a loose structure under hydrothermal conditional, which is desired for electrochromic application because the loose structure are effective in ion diffusion of the electrode. For the conventional polymerization, the pure PANI stacked to form layer agglomerates, which are not good for the transport of electrolyte ions in the electrode during electrochromic process. To further acquire the microscopic structure information of the PANI film, AFM observation was performed. As displayed in Fig. 1c,d, PANI nanofiber aggregation uniformly coated the whole surface of the FTO substrate, which is well consistent with the SEM results. The root-mean-square(RMS) surface roughness values obtained of 43.3 nm for the PANI film. Roughness values were obtained by sampling surface areas of 1 μm × 1 μm at three randomly selected locations on the sample. Therefore, as confirmed by the above SEM and AFM results, the PANI film has been successfully fabricated via a simple hydrothermal growth.

The FT-IR spectrumis shown in Fig. 2a. The two characteristic peaks at 1643 and 1552 cm^{-1} can be assigned to the stretching vibration of quinoid ring and benzenoid ring, respectively. The band at 1405 cm^{-1} attributes to C-H stretching vibration with aromatic conjugation. The peak at 1119 cm^{-1} results from the N = Q = N (Q denotes quinoid ring) stretching mode and is an indication of electron delocalization in PANI. The peak near 3213 cm^{-1} corresponds to the hydrogen-bonded N-H stretching vibration. The absorption around 884 cm^{-1} is due to the bending vibrations of the C-H bonds within the 1,4-disubstituted aromatic ring. The relatively strong peaks at 779cm^{-1}can be assigned to 1,3-coupling of the aromatic ring, indicates that the sample have the branched chain oligomers structures [27,28].

Raman spectra of the sample was recorded in order to confirm that PANI was formed, as shown in Fig. 2b. The spectrum of the neat polyaniline presents the following bands: 1624 cm^{-1} (νC–C of the benzene rings), 1578 cm^{-1} (νC=C of the quinoid rings), 1514 cm^{-1}(νC=H^+ of the quinoid protonated di-imine units), 1481 cm^{-1}(νC=N of the quinoid non-protonated diimine units), 1335 and 1315 cm^{-1} (νC—N^+, characteristic band of the polaron radical cation), 1256 cm^{-1} (νC–N of benzenoid and quinoid rings), 1193 and 1168 cm^{-1} (C–H bending of the benzenoid andquinoid rings, respectively) [29,30]. The bands at 405 cm^{-1} related to the C–H deformation, the band at 586 cm^{-1} attributed to the amine deformation, and the band at 514 cm^{-1} ascribed to the C-N-C torsion were also observed. The FTIR and Raman results indicated that the polymer film synthesized by hydrothermal method is identical to the conventional PANI.

The electrochemical properties of the as-synthesized PANI film were measured using a three-electrode electrochemical cell. Fig. 3a shows the cyclic voltammetry (CV) curves of the PANI film with scan rate of 10, 20, 30, 40, 50 and 100 mV s^{-1}, which was recorded between −0.3–1.4 V. The CV curves were attributed to the lithium-ion intercalation into the PANI electrode and the deintercalation process. The CV curves exhibited two pairs of redox peaks of PANI. The first pair of redox peak (c_1/a_1) can be attributed to the transformation between leucoemeraldine state (LES) and emeraldine states (ES) of PANI, and the second pair of redox peak (c_2/a_2) is ascribed to the transformation between ES and pernigraniline states (PNS). With the increasing of the scan rate, the LES to ES and ES to PNS transition peaks of PANI film shift to the positive direction, while the PNS to ES and ES to LES transition peaks shift to the negative direction. This indicates that the electrochemical redox reaction is a kinetic process determined by the conductivity and ion diffusion ability of the PANI. A nearly linear relationship between CV peak current density and square root of the scan rate can be found for PANI film as shown in Fig. 3b. The gradually increased peak current densities with increasing of scan rate suggest that the electrochemical process of PANI film are diffusion-controlled which are consistent with the previous results [16].

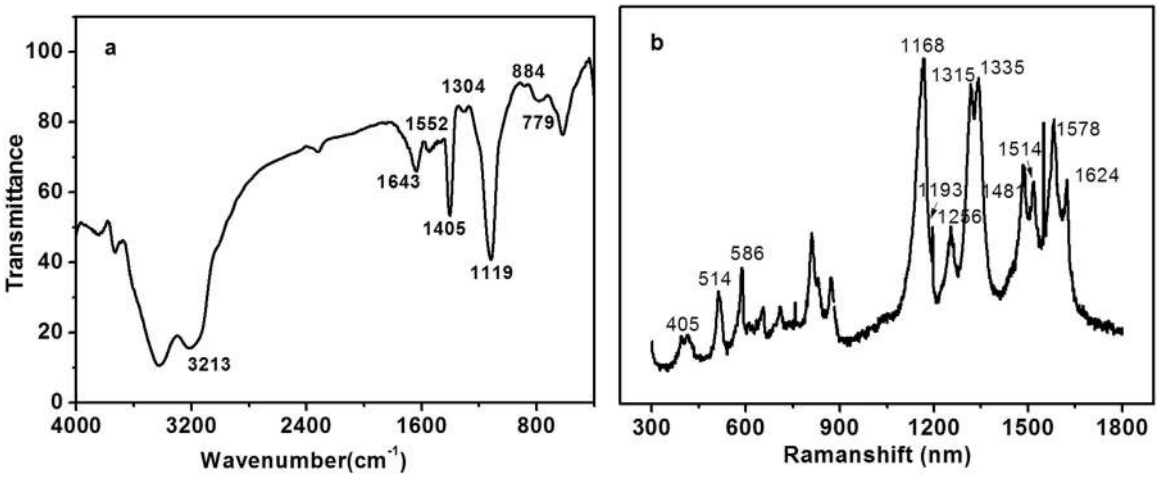

Fig. 2. (a) FTIR and (b) Raman spectrum of the as synthesized PANI film.

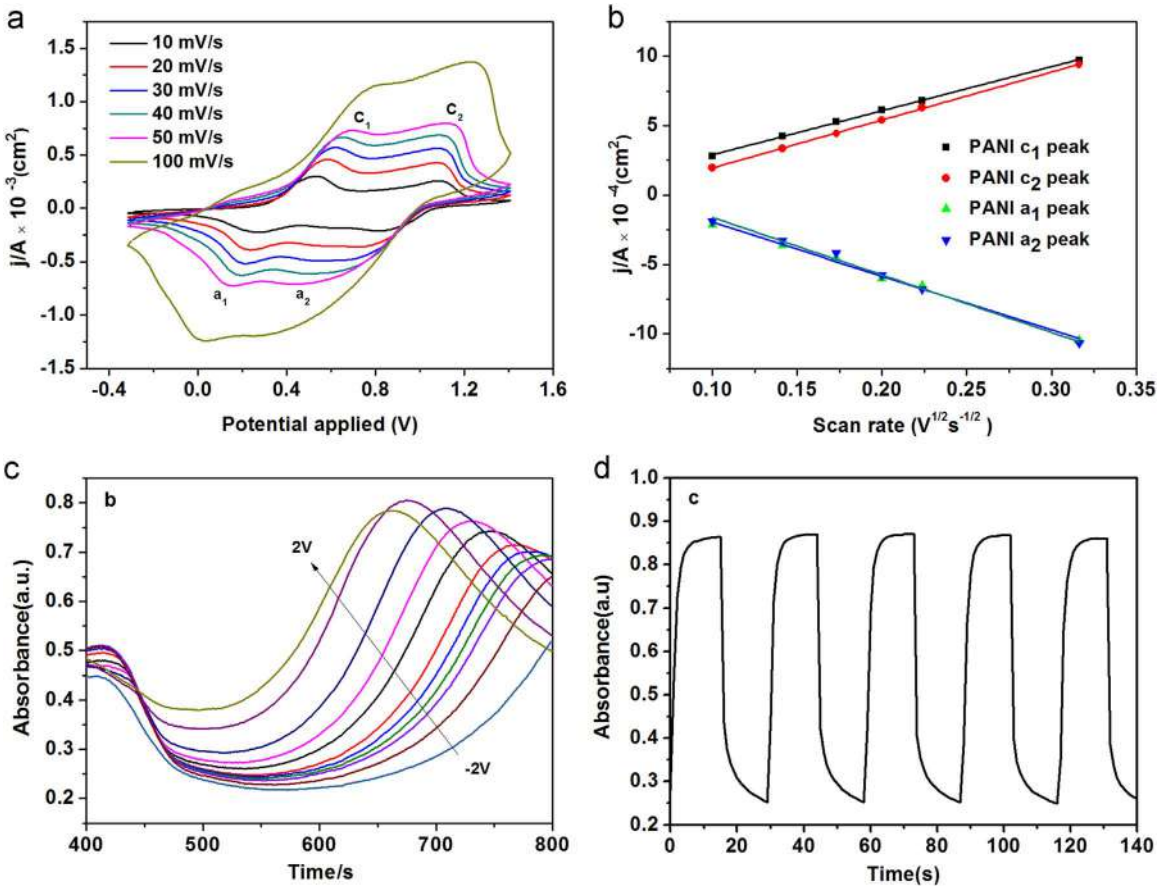

Fig. 3. (a) Cyclic voltammetry plots of the PANI film. (b) Plots of peak current density versus square root of the scan rate (c) Absorption spectra in the visible range for electrochromic devices with PANI layer as electrochromic layer. (d) Optical absorbance at λ_{max} for the devices with PANI film as the electrochromic layer, measured at −2.0/1.8 V with an absorbance wavelength of 670 nm.

The electrochromic properties of PANI films on FTO glass are studied by in-situ measuring the optical absorbance of device in the visible region from 400 to 800 nm with various potentials from −2.0 V to +2.0 V as shown in Fig. 3c. With applying the negative and positive potentials, all of the π-π* transition peaks of PANI shift to the long and short wavelength direction, respectively. When the applied negative potential is higher enough (< −2.0 V), the π-π* transition peak moves into near infrared region. In this case, the PANI film exhibits a relatively transparent color (light yellow). When the applied positive potential is higher enough (> 2.0 V), π-π* transition peak is located at about 700 nm and the PANI film exhibits blue color. The major electrochromic property, optical contrast is defined as the maximum absorbance difference between the coloration state and the bleaching state. It is obvious that the optical contrast under +1.8 V/−2.0 V potential increases from 0.56 for PANI film. The optical contrast in this study is larger than the reported optical contrast values of PANI composite synthesized by chemical polymerization in the literature [16,31–33]. The loose structure of the PANI which provides enhanced electrode/electrolyte interface contact and facilitate the rapid transport of electrolyte ions in the electrode during electrochromic process.

Besides of the optical contrast, the switching speed is another important parameter for judging the electrochromic properties of materials. The switching speed or the responding time is how fast the electrochromic materials response with the potential applied and exhibits their optical feature, which is related to the material nature and size of anion and cation in electrolyte. Fig. 3d displays the optical absorbance at 670 nm for the PANI film on FTO substrate under the step potential oscillating between +1.8 and −2.0 V with 20 s interval. The coloration and bleaching time of PANI film can be estimated according to the time needed for achieving 90% of their total absorbance changes. The coloration time is 3.1 s, while the bleaching time is 4.7 s. The excellent interfacial contact between PANI and FTO glass facilitates fast transportation of ions throughout the whole electrode matrix which are attributed to their unique loose structure.

4. Conclusion

In summary, PANI films are assembled directly on a FTO glass substrate via a facile hydrothermal method. The structure, electrochemical and electrochromic studies based on this film are presented. The PANI film shows good coloration/bleaching switching characteristics. There is a good prospect of applying this hydrothermal PANI film in smart window and electronic papers.

Acknowledgments

This work was supported by the National Natural Science Foundation of China (NSFC, No. 51503169, 51373134).

References

[1] S. Günes, H. Neugebauer, N.S. Sariciftci, ChemInform 107 (31) (2007) 1324–1338.
[2] J. Yang, Y. Liu, S. Liu, L. Li, C. Zhang, T. Liu, Mater. Chem. Front (2017), http://dx.doi.org/10.1039/C6QM00150E.
[3] T. Sen, S. Mishra, N.G. Shimpi, RSC Adv. 6 (2016) 42196–42222.
[4] Z. Tian, H. Yu, L. Wang, M. Saleem, F. Ren, P. Ren, Y. Chen, R. Sun, Y. Sun, L. Huang, RSC Adv. 4 (2014) 28195–28208.
[5] J. Lai, Y. Yi, P. Zhu, J. Shen, K. Wu, L. Zhang, J. Liu, J. Electroanal. Chem. 782 (2016) 138–153.
[6] S. Xiong, F. Yang, H. Jiang, J. Ma, X. Lu, Electrochim. Acta 85 (2012) 235–242.
[7] S. Xiong, Y. Shi, J. Chu, M. Gong, B. Wu, X. Wang, ElectrochimActa 127 (2014) 139–145.

[8] L. Ma, M. Gan, G. Fu, M. Jin, Y. Lei, P. Yang, M. Yan, J. Power Sources 340 (2017) 22–31.
[9] X. Feng, H. Li, J. Song, L. Wang, R. Liu, W. Zeng, Z. Huang, Y. Ma, L. Wang, Nanoscale (2016), http://dx.doi.org/10.1039/C6NR07921K.
[10] H. Rao, M. Chen, H. Ge, Z. Lu, X. Liu, P. Zou, X. Wang, H. He, X. Zeng, Y. Wang, BiosensBioelectron 87 (2017) 1029–1035.
[11] T. Yang, L. Meng, J. Zhao, X. Wang, K. Jiao, ACS Appl. Mater. Interfaces 6 (2014) 19050–19056.
[12] S. Abdulla, T.L. Mathew, B. Pullithadathil, Sens. Actuators B: Chem. 221 (2015) 1523–1534.
[13] B.C. Sherman, W.B. Euler, R.R. Force, J. Chem. Educ. 71 (1994) A94.
[14] C.W. Hu, T. Kawamoto, H. Tanaka, A. Takahashi, K.M. Lee, S.Y. Kao, Y.C. Liao, K.C. Ho, J. Mater. Chem. C 4 (2016) 10293–10300.
[15] P. Jia, A.A. Argun, J. Xu, S. Xiong, J. Ma, P.T. Hammond, X.H. Lu, Chem. Mater. 21 (2009) 4434–4444.
[16] S. Xiong, J. Wei, P. Jia, L. Yang, J. Ma, X. Lu, ACS Appl. Mater. Interfaces 3 (2011) 782–788.
[17] W. Zhang, W. Ju, X. Wu, Y. Wang, Q. Wang, H. Zhou, S. Wang, C. Hu, Appl. Surf. Sci. 367 (2016) 542–551.
[18] X. Wu, W. Zhang, Q. Wang, Y. Wang, H. Yan, W. Chen, Synth. Met. 212 (2016) 1–11.
[19] L. Fu, S.J. You, G.Q. Zhang, F.L. Yang, X.H. Fang, Z. Gong, Biosens. Bioelectron. 26 (2011) 1975–1979.
[20] H. Wang, J. Lin, Z.X. Shen, J. Sci.: Adv. Mater. Devices 1 (2016) 225–255.
[21] J.F. Felix, R.A. Barros, W.M.D. Azevedo, E.F.D. Silva, Synth. Met. 161 (2011) 173–176.
[22] J. Cho, K.H. Shin, J. Jang, Thin Solid Films 518 (2010) 5066–5070.
[23] C. Laslau, D.E. Williams, B. Kannan, J.T. Sejdic, Adv. Funct. Mater. 21 (2011) 4607–4616.
[24] X. Zhu, K. Hou, C. Chen, W. Zhang, H. Sun, G. Zhang, Z. Gao, High. Perform. Polym. 27 (2) (2015) 207–216.
[25] L. Pan, L. Pu, Y. Shi, T. Sun, R. Zhang, Y. Zheng, Adv. Funct. Mater. 16 (2006) 1279–1288.
[26] B. Baumgartner, M.J. Bojdys, M.M. Unterlass, Polym. Chem. 5 (2014) 3771–3776.
[27] Y.S. Zhang, W.H. Xu, W.T. Yao, S.H. Yu, J. Phys. Chem. C 113 (2009) 8588–8594.
[28] J. Fei, Y. Cui, X. Yan, Y. Yang, Y. Su, J. Li, J. Mater. Chem. 19 (2009) 3263–3267.
[29] L. Zhang, M. Wan, Adv. Funct. Mater. 13 (2003) 815–820.
[30] S.X. Xiong, Y.J. Yu, J. Chu, M. Gong, B.H. Wu, X.Q. Wang, Electrochim. Acta 127 (2014) 139–145.
[31] E.M. Erro, A.M. Baruzzi, R.A. Iglesias, Polymer 55 (2014) 2440–2444.
[32] W. Zhang, W.X. Ju, X. Wu, Yan Wang, Q. Wang, H. Zhou, S. Wang, C. Hu, Appl. Surf. Sci. 367 (2016) 542–551.
[33] C.L. Lin, L.J. Liao, Sol. Energy Mater. Sol. Cells 145 (2016) 54–60.